Extension of Range Migration Algorithm for Airborne SAR Data Processing

Hee-Sub Shin, Won-Gyu Song, Jun-Won Son, Yong-Hwan Jung, and Jong-Tae Lim

Dept. of EECS and Radiowave Detection Research Center, KAIST. Daejeon, Korea
Tel: +82-42-869-3441; Fax: +82-42-869-3410
Email: ahwahs@kaist.ac.kr, w_song@kaist.ac.kr, couldbe@eeinfo.kaist.ac.kr, jungyonghwan@kaist.ac.kr, jtlim@stcon.kaist.ac.kr

Abstract: Several algorithms have been developed for the data processing of spotlight synthetic aperture radar (SAR). In particular, the range migration algorithm (RMA) does not assume that illuminating wavefronts are planar. Also, a high resolution image can be obtained by the RMA. This paper introduces an extension of the original RMA to enable a more efficient airborne SAR data processing. We consider more general motion and scene than the original RMA. The presented formulation is analyzed by using the principle of the stationary phase. Finally, the extended algorithm is tested with numerical simulations using the pulsed spotlight SAR.

Keywords: Spotlight Synthetic Aperture Radar, Range Migration Algorithm

1. Introduction

A SAR is a powerful remote sensing technique that allows the generation of microwave images of the earth's surface, independently of weather condition and sun illumination. In particular, the spotlight SAR is able to obtain a high geometric azimuth resolution by steering the radar antenna beam during the raw data acquisition interval, to always illuminate the same area on the ground. This azimuth steering allows the sensor to obtain a longer synthetic array without increasing the real antenna azimuth size.

Several algorithms have been developed for the reconstruction of spotlight SAR raw data. Each has its own advantages and shortcomings. Carrara et al. [1] give a comprehensive review of the polar format algorithm (PFA), chirp scaling algorithm (CSA) and range migration algorithm (RMA). The RMA is sometimes called the ω-k algorithm [2]. First, the PFA is well known for processing spotlight SAR data. This algorithm involves the assumption that the spherical wavefronts of the radar pulses can be approximated by planar wavefronts around the scene center. While these approximations are often quite good for small target scenes imaged by airborne platforms, for larger scenes, the approximations lead to errors in parts of the scene far away from the scene center. The Extended Chirp Scaling (ECS) algorithm is proven to be very powerful in the algorithm's ease of implementation but does not provide the exact solution in the focusing procedure due to approximations made in chirp scaling processing. As a result of this, the introduced phase errors are limiting the maximum achievable along track resolution [4]. The RMA can reconstruct exactly the reflectivity function of targets. Also, this algorithm has the advantages that range cell migration (RCM) can be compensated for all targets within the scene and that it can handle high squint angles and wide apertures accurately [1]-[3]. However, since the RMA assume that the SAR sensor traverses a straight-line flight path parallel to the azimuth axis, there are limitations in performing a real motion of airborne SAR.

This research was supported by the Agency for Defense Development, Korea, through the Radiowave Detection Research Center at Korea Advanced Institute of Science & Technology.

In this paper, we propose an extension of the original RMA to enable a more efficient method of raw data processing. Moreover, in order to test processing algorithms, we design a raw signal simulator. In the simulator, the SAR raw signal is computed via a superposition integral in which the reflectivity map is weighted by the pulsed SAR system.

2. Signal Model

The geometry model in Figure 1 provides the basis for a simple SAR signal model to analyze the RMA. The SAR sensor travels an area during a synthetic aperture length L. The radar has a 2-D planar aperture. Also, the radar transmits and receives pulses at a fixed pulse repetition interval to maintain uniform spatial sampling along the flight path. Also, we assume that small deviation in the range direction exists and the airborne SAR is equipped with exact global positioning system (GPS).

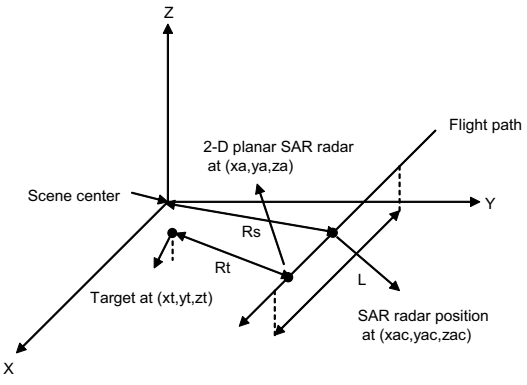

Figure 1: Imaging geometry model

The X axis of this system is parallel to the azimuth direction. The fixed slant range distance between the center position of the flight path, i.e. (x_{ac}, y_{ac}, z_{ac}) and the scene center is R_s. Point target analysis assumes that there is a single point target within the imaged scene at coordinates (x_t, y_t, z_t). The distance R_t between the radar and this target varies as a function of the SAR sensor position.

We introduce the extended RMA for a SAR system us-

ing a linear FM (chirp) waveform. In the geometry model of Figure 1, the SAR system transmits pulses at position (x_a, y_a, z_a) along the flight path. If there is a point target located at (x_t, y_t, z_t) with reflectivity function $\rho(x_t, y_t, z_t)$, then the received signal is

$$s_r(n,t) = \rho(x_t, y_t, z_t) e^{j2\pi f_c (t - \frac{2R_t}{c})} e^{j\pi\gamma(\hat{t} - \frac{2R_t}{c})^2} \quad (1)$$

The quantity f_c represents the center transmit frequency, c is the speed of microwave, γ is the chirp rate and the symbol $\hat{t}$ is defined by $\hat{t} = t - nT$, where n is discrete pulse number and T is the period between successive pulse transmissions. Also, R_t is the range between the radar and the point target, i.e.,

$$R_t = \sqrt{(x_a - x_t)^2 + (y_a - y_t)^2 + (z_a - z_t)^2} \quad (2)$$

We use the following reference signal with the constant reference range R_s

$$s_{ref}(n,t) = e^{j2\pi f_c (t - \frac{2R_s}{c})} e^{j\pi\gamma(\hat{t} - \frac{2R_s}{c})^2} \quad (3)$$

If we demodulate the received signal (1) using the reference signal (3), the resulting signal is

$$s(x_a, y_a, z_a, \hat{t}) \quad = \quad \rho(x_t, y_t, z_t) e^{j\Phi(x_a, y_a, z_a, \hat{t})} \quad (4)$$

with $\Phi(x_a, y_a, z_a, \hat{t}) = -\frac{4\pi\gamma}{c}(\frac{f_c}{\gamma} + \hat{t} - \frac{2R_s}{c})(R_t - R_s) + \frac{4\pi\gamma}{c^2}(R_t - R_s)^2$ Also, since the residual video phase term can be removed by the preprocessing of range deskew, we obtain the following phase

$$\Phi(x_a, y_a, z_a, k_r) = -k_r(R_t - R_s) \quad (5)$$

where $k_r = \frac{4\pi\gamma}{c}(\frac{f_c}{\gamma} + \hat{t} - \frac{2R_s}{c})$. For simplicity, we assume the backscattered amplitude and phase characteristic of the point target do not vary with frequency and other effect.

3. Main Results

3.1. Overview of Extended RMA

This section provides a simple overview of the extended RMA and illustrates its basic operation. The block diagram in Figure 2 provides the basis for image reconstruction processing via the extended RMA. After the conjugate operation, we perform the 2-D Fourier transform with respect to x_a and z_a for the collected SAR signal. Thereafter, we use the matched filter to correct all range curvature of targets. Also, after Stolt interpolation, we reconstruct the complex image via 3-D inverse FFT with upsampling to avoid aliasing due to compression.

3.2. 2-D Fourier Transform Analysis

From (4) and (5), we obtain

$$s(x_a, y_a, z_a, k_r) = \rho(x_t, y_t, z_t) e^{-jk_r(R_t - R_s)} \quad (6)$$

Also, from the conjugate operation of (6), we obtain the following equation

$$s_1(x_a, y_a, z_a, k_r) = \rho(x_t, y_t, z_t) e^{jk_r(R_t - R_s)} \quad (7)$$

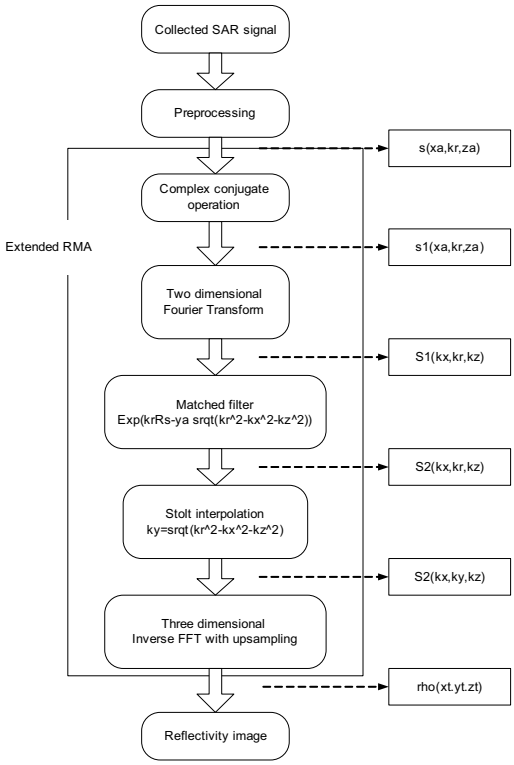

Figure 2: Block diagram of extended RMA

The 2-D Fourier transform of (7) with respect to x_a and z_a yields

$$S_1(k_x, k_r, k_z) = \int\int s_1(\cdot) e^{-(jk_x x_a + jk_z z_a)} dx_a dz_a \quad (8)$$

To evaluate (8), using the method of stationary phase [5], we determine the stationary points of its phase. The phase function φ corresponds to

$$\varphi(x_a, y_a, z_a, k_r) = k_r R_t - k_x x_a - k_z z_a \quad (9)$$

where $R_t = \sqrt{(x_a - x_t)^2 + (y_a - y_t)^2 + (z_a - z_t)^2}$.
Substituting R_t into (9) and equating the first derivative to zero gives

$$\frac{\partial\varphi(x_a, y_a, z_a, k_r)}{\partial x_a}(x_0, z_0) = \frac{k_r(x_0 - x_t)}{R_{t0}} - k_x = 0 \quad (10)$$

$$\frac{\partial\varphi(x_a, y_a, z_a, k_r)}{\partial z_a}(x_0, z_0) = \frac{k_r(z_0 - z_t)}{R_{t0}} - k_z = 0 \quad (11)$$

where $R_{t0} = \sqrt{(x_0 - x_t)^2 + (y_a - y_t)^2 + (z_0 - z_t)^2}$.
Solving (10) and (11) for x_0 and z_0 respectively, yields

$$x_0 \quad = \quad \frac{k_x(y_a - y_t)}{\sqrt{{k_r}^2 - {k_x}^2 - {k_z}^2}} + x_t \quad (12)$$

$$z_0 \quad = \quad \frac{k_z(y_a - y_t)}{\sqrt{{k_r}^2 - {k_x}^2 - {k_z}^2}} + z_t \quad (13)$$

as the stationary points.
The phase of $S_1(k_x, k_r, k_z)$ is

$$\Phi_{rma}(k_x, k_r, k_z) = k_r R_t - k_x x_a - k_z z_a - k_r R_s \quad (14)$$

Substituting the value x_0 and z_0 for x_a and z_a in (14), we obtain

$$\begin{aligned}\Phi_{rma}(\cdot) &= -k_x x_t - k_z z_t - k_r R_s \\ &\quad +(y_a - y_t)\sqrt{{k_r}^2 - {k_x}^2 - {k_z}^2} \end{aligned} \quad (15)$$

after some manipulation.
Also, we assume that the amplitude factor is suppressed in the reflectivity function. Thus, we obtain the following signal

$$S_1(k_x, k_r, k_z) = \rho(x_t, y_t, z_t)e^{j\Phi_{rma}} \quad (16)$$

3.3. Matched Filtering Analysis

The second step is a phase compensation to the 2-D transformed signal. The matched filter is defined as follows

$$\Phi_{mf}(k_x, k_r, k_z) = -y_a\sqrt{{k_r}^2 - {k_x}^2 - {k_z}^2} + k_r R_s \quad (17)$$

This matched filtering operation corrects the range curvature of all targets at the same range as scene center.

3.4. Stolt Interpolation Analysis

A change of variables, known as the Stolt interpolation is defined as follows

$$k_y = \sqrt{{k_r}^2 - {k_x}^2 - {k_z}^2} \quad (18)$$

After application of the Stolt interpolation, the signal becomes

$$\begin{aligned} S_2(k_x, k_y, k_z) &= S_1(k_x, k_r, k_z) \times e^{\Phi_{mf}(k_x, k_r, k_z)} \\ &= \rho(x_t, y_t, z_t)e^{-j(k_x x_t + k_y y_t + k_z z_t)} \end{aligned} \quad (19)$$

Thus, if we consider a scene with a distributed target, we can obtain the following desired signal

$$S_{rma}(\cdot) = \int\int\int \rho(\cdot)e^{-j(k_x x_t + k_y y_t + k_z z_t)}dx_t dy_t dz_t \quad (20)$$

Thus, from (20), if we perform compression via a three-dimensional inverse FFT, we can reconstruct the scene image.

4. Simulation Results

We tested the extended RMA with simulated data and compared the results with the original RMA. The basic simulation parameters are as follows:

- Center frequency (f_c) : 10^{10}Hz
- Synthetic aperture length (L) : 100m
- Bandwidth (B) : 133.5×10^6Hz
- Pulse repetition frequency (PRF) : 1000Hz
- Platform velocity (v) : 400m/s
- Pulse width (T_P) : 10^{-6}sec
- Chirp rate (γ) : B/T_p
- Speed of light (c) : 2.99792458×10^8m/s
- Complex sampling frequency (F_s) : 185.0×10^6Hz

As shown in Figure 3, for simplicity, there are five point targets with the same reflectivity magnitudes and $z_t = 0$ in the scene. Also, z_{ac} is a constant value $2000m$. Also, due to high atmospheric turbulence, we assume that there are $2m$ deviation in the range direction from the position $x_a = L/2$ (case 1) and $1 \sim 3m$ deviations in the same direction from the position $x_a = L/4, L/2$ and $3L/4$ (case 2). We show some simulation results to verify the feasibility of our algorithm. As shown in Figs. 4−5, the extended RMA yields a better response as compared to the original RMA. Also, the targets can be mixed in the original RMA. However, as further works, we need to study the sidelobe reduction of the extended RMA.

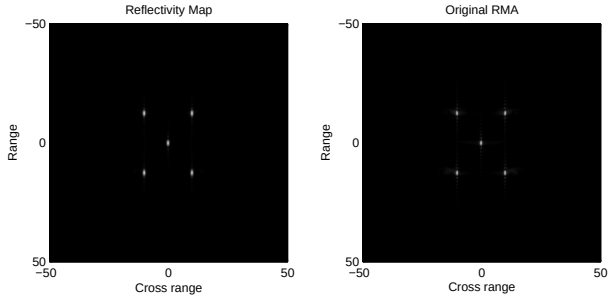

Figure 3: Platform motion with constant y_a

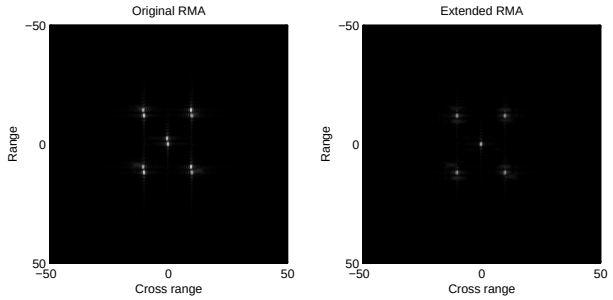

Figure 4: Platform motion with variable y_a (case 1)

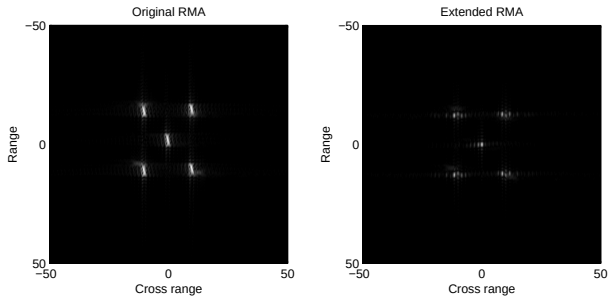

Figure 5: Platform motion with variable y_a (case 2)

5. Conclusions

In this paper, the 2-D original RMA with a straight-line motion of platform was extended. That is, we introduced the 3-D SAR reconstruction algorithm with more general flight path. Also, some additional terms were formulated by the method of stationary phase. Using the pulsed SAR simulator, we showed advantages of the extended RMA. Also, we will study the sidelobe reduction problem and motion error of other directions.

References

[1] W. G. Carrara, R. S. Goodman, and R. M. Majewski, *Spotlight Synthetic Aperture Radar Signal Processing Algorithms*, Artech House, 1995.

[2] C. Prati, A. Guarnieri, and F. Rocca, "Spotlight mode SAR focusing with the ω-k technique," *Proc. IGARSS*, Espoo, Finland, pp. 631-634, June 1991.

[3] A. Reigber, A. Potsis, E. Alivizatos, N. Uzunoglu, and A. Moreira, "Wavenumber domain SAR focusing with integrated motion compensation," *Proc. IGARSS*, 2003.

[4] A. Moreira, J. Mittermayer, and R. Scheiber, "Extended chirp scaling algorithm for air- and spaceborne SAR data processing in stripmap and ScanSAR imaging modes," *IEEE Transactions on Geoscience and Remote Sensing*, Vol. 34, No. 5, pp. 1123-1136, Sep. 1996.

[5] Born, M., and E. Wolf, *Principles of optics : electromagnetic theory of propagation, interference and diffraction of light*, Cambridge University Press, 1999.